2-D Comparitive Performance Analysis on a Numerically Computed Aerospike Nozzle Plug

P A Chandru*, Kanishka Awasthi[1], Sri Sanjay[2]

*Corresponding Author Email: chandrupa.aeroin@gmail.com

AEROIN SPACETECH PRIVATE LIMITED

---***---

Abstract - This comparative analysis paper focusses on the rudiments of aerospike plug design and related performance analysis for the nozzle performing at an altitude of 7000 m. The plug nozzle has been derived using preliminary thermodynamic and aerodynamic theory as studied from the reference papers, which are then used as the basic building blocks of an elaborate MATLAB code. The code utilises inputs such as number of characteristic Mach lines, exit area of the nozzle, percentage of truncation length, and exit Mach value. The main use of the code is to get a numerically calculated contour profile of the nozzle plug. This contour profile is then studied and filtered in the 3-D CAD software CATIA V5, and converted to half symmetry which is then imported in ANSYS Fluent (*version 2024 R1 -student*) for further CFD analysis. The main aim of this paper is to validate certain input criteria already tested once in a reference paper, with small modulations in the design of annular nozzle to see variations in the output results.

1.INTRODUCTION

Space technology has seen a steady rise in its design development in the past decade or so. The amount of time, energy and innovation which is mostly spent in making these technologies reusable, environment adaptive and cost effective is worthy of praise. A significant surge in the design modulation of propulsion systems is also seen with a specific motive of trying new variations in renewed types such as aerospike propulsion systems. Aerospike propulsion systems came around during the 1960's but as a result of issues arising from thermal and strength perspectives, these nozzles were scarred for further research. These types of propulsion system nozzles were theorised for Space shuttle main engines as one of the main contenders, however no such commercial based application is seen so far.

An aerospike nozzle system has got 2 main parts: the annular nozzle ring equipped with thrusters, and the aerospike "plug" which protrudes up to a truncated length thereby ensuring a base bleed at the end of the truncation, hence improving the overall thrust performance of the associated system. Such types of nozzle assemblies are used wherever an altitude compensation is required, that is, changing the thrust output and the orientation at varying altitudes in order to account for variable surrounding ambient pressure which in turn affects the thrust force.

Thrust Analysis in aerospike nozzle:

There are three types of thrust forces which are generated in an aerospike nozzle system. The same are mentioned below along with their adjoined formulations:

(a) *Force due to thrusters present in Toroidal chamber (annular nozzle base)*: This includes the main primary exhaust being let out at an angle theta (θ) to the main aerospike plug axis. It is given using the formula:

$$F_{thrusters} = (m\,V_{exit} + (P_{exit} - P_{free-stream})A_{exit})cos\theta$$

(b) *Forces acting at the centre-body of the spike plug:* As the exhaust gases in case of a nozzle system always have a tendency to expand against the nozzle walls due to their high kinetic energy by virtue of the exhaust pressure difference, these gases due to the absence of a surrounding bell nozzle wall as in case of a conventional nozzle, strive to expand against the centre-body surface of the plug. The relation for same is given as:

$$F_{centre-body} = \int_{0}^{A_{centre-body}} (P_{centre-body} - P_{free-stream})dA$$

(c) *Force at the spike plug base:* As a result of truncation, the plug has a flat base at the end of the spike which accounts for the base force generated due to the circulation of the subsonic secondary flow. The formula for this is given as:

$$F_{base} = (P_{base} - P_{free-stream})A_{base}$$

Finally, the net thrust imparted by the aerospike is given as the sum of the above 3 forces as:

$$F_{Total} = F_{thrusters} + F_{centre-body} + F_{base}$$

Exhaust flow analysis in aerospike engines:

For a given aerospike nozzle contour design, a typical exhaust flow consists of a primary supersonic exhaust mixture of the combust gases, an outer free jet boundary, an oblique shock

envelope created by trailing shocks, an inner shear layer (which marks the transition of supersonic primary flow to subsonic flow), and a circulating subsonic base flow at the flat end of truncation.

As a general characteristic feature, the outer jet boundary layer is allowed to freely expand to the outside ambient pressure, whereas the characteristic Mach lines making up the expansion wave extrapolate from the thruster lips, onto the spike plug contour, get reflected and progress towards the outer-boundary line. Further reflections from the outer jet boundary layer, lead to the formation of compression waves which coalesce with one another to form oblique shock waves interacting with the outer primary flow and hence with the ambient pressure. The outer primary exhaust flow and the inner subsonic circulating base flow are separated by a shear layer which marks a transition between the two.
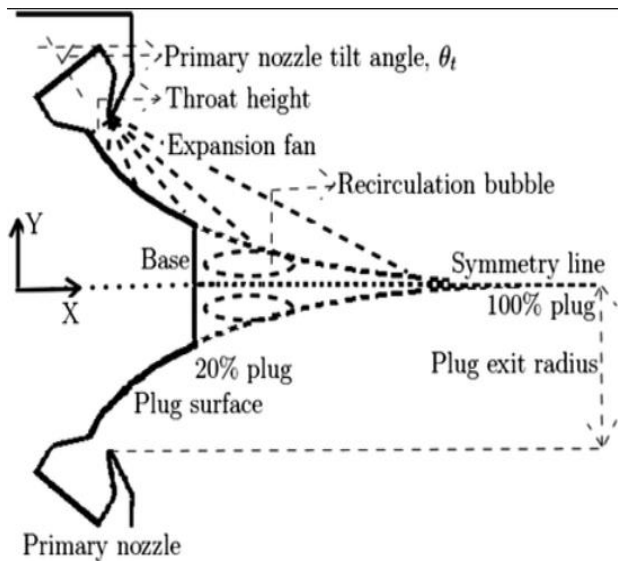
Figure 1: Schematic of an aerospike nozzle exhaust flow over truncated plug

Altitude Compensation:

At low heights above sea level, the ambient pressure is high, hence the primary exhaust flow along with the outer jet boundary are compressed more to the centre-body surface of the plug. This in turn increases the centre-body force component of thrust. Also the compression waves in such scenario are elongated horizontally in order to form the subsonic wake region impacting the shear layer more, thereby increasing the circulation of the base flow and hence increasing the base force component of thrust as well.

The ambient pressure at higher altitudes on the other hand is comparatively lower, thereby allowing the compression waves to skew closer to one-another and hence decreasing the proximity of the outer primary flow exhaust around the contour wall allowing it to expand further outwards. This in turn decreases the centre-body component of thrust, which continues to become constant with the surrounding pressure, whereas the base flow circulation pressure, which also decreases, still remains a function of the said ambient pressure. This continues to decrease until finally reaching a constant value with an enclosed wake region by the oblique shocks.
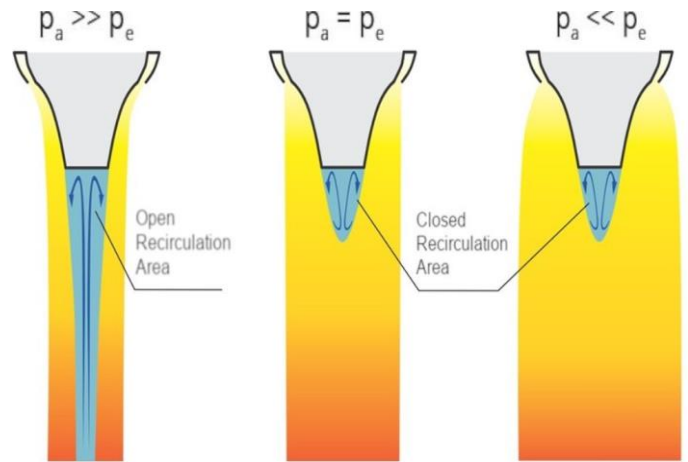
Figure 2: Over, optimum, and under expansion in an aerospike nozzle plug

2.LITERATURE REVIEW

Chutkey, Kiran et al. (2017) discusses the fact that aerospike nozzle's altitude compensating features and shorter nozzle length than a normal contoured CD nozzle make it a viable option for next-generation launch vehicle propulsion systems. Things in subsonic flow behave aerodynamically very differently from those in supersonic flow. A passive altitude adaptable device designed for single stage to orbit (SSTO) applications is the plug nozzle. Because of its altitude adaptation, it can operate over a wide variety of pressure ratios that correspond to significantly varied elevations. As a result, it displays some of the most fascinating and intricate flow physics seen in gas dynamics.

Under design conditions, the full-length plug nozzle in ***Chutkey, Kiran et al. (2017)*** displays a continuously expanding flow; under off-design conditions, however, the core jet flow displays wave interactions. Conversely, the practically attainable truncated plug nozzle demonstrates the intricacies of both the base flow and its transition, as well as the interactions between waves within the core jet flow.

The design profile of an aerospike nozzle contour and its optimization are discussed by ***C.H. Wang, Y. Liu, L.Z. Qin, et al. (2009).*** Both experimental and numerical results are obtained from this process. The primary nozzle contour and the plug contour are the two primary components of the overall nozzle geometry. While the plug contour is the product of estimating a parabola profile and a polynomial equation (3rd order) profile, the primary contour is designed by approximating two circular arcs and one parabola. Following investigations on three different types of aerospike nozzles distinguished by N-cell tile number, experimental results were obtained for a 1-cell linear tile, a 3-cell aerospike, and a 6-cell tile-shaped. All are having a comparable aerospike nozzle contour profile, but differing in nozzle thruster number, orientation, and location.

Only one type of analysis is employed per experiment trial in ***C.H. Wang, Y. Liu, L.Z. Qin, et al.'s (2009)*** experimental analysis, which focuses on the operation conditions in addition to three distinct cell number (N)-tile classifications by incorporating both cold-flow and hot-firing criteria.

Extremely pressurized air was used in the pressure feed system supply for the cold-flow analysis, while room-temperature propellant mixtures of O2 and H2 were employed for the hot-firing process. An igniter with detonation wave capabilities was used in the hot firing test. For puffing, nitrogen (N2) at high pressurization conditions was utilized.

For research involving numbers the flow calculations for the external flow of the plug nozzle and the internal flow of the primary nozzle were completed independently by *C.H. Wang, Y. Liu, L.Z. Qin, et al. (2009)*. The plug contour profile's inlet circumstances are determined by the flow conditions at the primary nozzle. Using the Lam–Bremhorst k–ε turbulent model, governing equations in the form of three-dimensional Reynolds averaged N–S equations are finally determined. The impact of ambient pressure is disregarded due to the very tiny primary nozzle area ratio. Lastly, validation results are achieved using both numerical and experimental methods. The experimental method provides data for plug wall pressure Pp, ambient pressure in the vacuum chamber/vessel Pa, and chamber pressure PC. The uncertainty error in total thrust production hold is less than 0.1%. The numeric yielded hot firing results on 3-cell tile shaped nozzles subjected to two different NPRs with efficiency reaching 95-96%. Cold flow analysis including the 6-cell tile and 1-cell linear nozzle gave efficiency of 92-93.5%.

In another paper referred, **M. Imran et.al, (2016)** shows a study proving that the altitude correction is essential for rocket propulsion, particularly for vehicles that are single-stage to orbit. Rocket dyne's aerospike nozzle, created in the 1950s, guarantees the best thrust performance for a variety of flight profiles. With the help of research, nozzle design has improved, with issues with density and air pressure. Experimental testing and CFD simulations can be used to improve aerodynamic efficiency and behaviours such that the efficiency will be increased in the aerospike engine. The utilization of altitude compensating nozzles in reusable SSTO vehicles decreases the economy. The least used nozzle and the annular nozzle, may be more effective and better in performance.

Dakka, S., & Dennison, O. (2021) talks about Rao's introduction of the bell nozzle contour in 1958, stating that rocket nozzle design has undergone critical changes. However, problems with over-expansion and flow separation make conventional nozzles less efficient. Rocket dyne's aerospike engines, created in the 1950s, provide enhanced performance and altitude compensating features. The optimization of aerospike engine designs and truncation lengths has been the focus of research employing numerical analysis and CFD simulations. When it comes to performance, linear aerospike engines are especially versatile and may outperform traditional bell nozzles. The development of space propulsion technologies is greatly aided by this research.

3. METHODOLOGY

The entire methodology has been broken down into three main stages: Numerical computation, CAD modelling/filtering, and 2-D domain meshing with associated CFD flow simulation. The original aerospike contour design which is considered from an input-initialisation point of view is the one mentioned in *Chutkey, Kiran et al. (2017)*, and thus a constant comparative modulation is provided and mentioned accordingly in the below mentioned detailed methodology. Following bulletins discuss the approach taken in each of the stages in a progressive manner in order to achieve the desired results:

(a) *Numerical Modelling and contour profile computation:*

MATLAB software was used to code the contour profile by utilizing certain essential inputs such as number of characteristic Mach lines, exit area of the nozzle, percentage of truncation length, and exit Mach value. These values were used along with various other intermediate step algorithms which were employed to fetch the necessary reference point of contour calculation.

Firstly, by using the exit Mach value, and the number of characteristic line inputs, an initial set of 'n' Mach values was prepared to be used in the contour plotting loops. Once this set was achieved, the other necessary values such as gamma (adiabatic gas constant), R (universal gas constant), etc. were defined.
The algorithm approach taken was the Angelino's simple approximation method as referenced from **Dakka, S., & Dennison, O. et.al, (2021**).
This method utilises the concepts of expansion ratio (A.R), Prandtl-Meyer angle (ν), Mach angle (μ), flow direction angle (α), characteristic line length (l), and the exit radius (r_e). The method strives to calculate the characteristic line length, along with the exit radius value (r_e), thereby using l/r_e as a dimensionless parameter to get the required x and y values of the contour profile by iterating the Mach values between '1' and exit Mach value, 'n' times.

The relations for calculating the above mentioned values, as there are found sequentially in the contour –plotting loop of the code, are formulated below:

$$A.R = \frac{1}{M}\left[\frac{2}{\gamma+1}\left[1 + \frac{\gamma-1}{2}M^2\right]\right]^{\frac{\gamma+1}{2(\gamma-1)}}$$

$$\nu(M) = \sqrt{\frac{\gamma+1}{\gamma-1}}\left[\tan^{-1}\sqrt{\frac{\gamma-1}{\gamma+1}(M^2-1)} - \tan^{-1}\sqrt{(M^2-1)}\right]$$

$$\mu = \sin^{-1}\frac{1}{m}$$

$$\alpha = \mu - \nu$$

$$l = \frac{r - r_e}{\sin\alpha}$$

$$X_{non-dim} = \frac{l}{r_e}\cos\alpha$$

$$Y_{non-dim} = \frac{l}{r_e}\sin\alpha$$

$$X_{contour} = X_{non-dim} * r_e$$

$$Y_{contour} = Y_{non-dim} * r_e$$

For our particular case we have slightly changed our approach by first calculating the full length of the plug profile for zero truncation using the above loop and then interpolating for the required truncation percentage using the original length as reference and then rerunning the loop for the given truncation. A very important parameter in the above mentioned loop is the non-dimensional base radius η_b, which takes 0 value for full plug length consideration and other values for various other truncation percentages as specified by the chart below.

η	Length (m)
0.5	1.80
0.4	2.27
0.2	2.99
0	3.67

Figure 3: Table for truncation values for different values of non-dim base radius

Finally, the resultant profile is plotted using MATLAB code and then imported into excel, followed by a final import into CATIA V5 using excel **macros** for further adjustments. Extra heed is given to the parabolic curvature of the profile obtained which is constantly compared with the one designed in *Chutkey, Kiran et al. (2017).* Here the skewness from the referred curvature makes a significant impact on flow simulation results.

4. RESULT
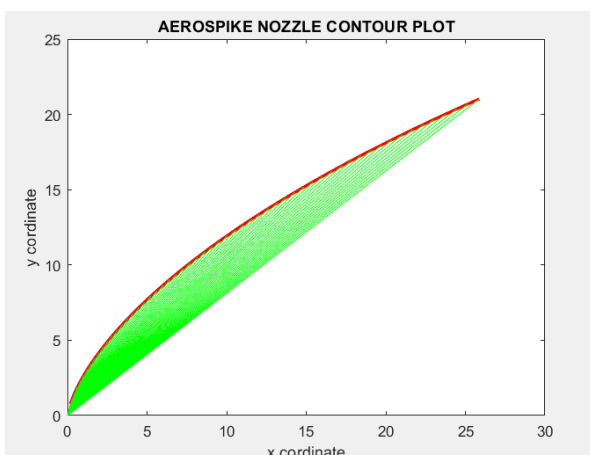
Figure 4: Aerospike Contour Profile Plot (as obtained from MATLAB)

*NOTE: The red curve signifies the actual profile obtained and the green lines signify the   characteristic line/characteristic line lengths.

Inputs given into the MATLAB code:

PARAMETER	VALUE
Number of characteristic lines	60
Exit Mach number	2.09
Exit area of nozzle	84.3655 mm^2
Percentage of truncation	20 %
A_e/A_t	1.82118
gamma	1.4
R (specific gas constant)	287.05 J.Kg^{-1}.k^{-1}
g (acceleration due to gravity)	9.81 m/s^2

(b) 2-D Contour filtration/surface hex domain formation in CATIA V5:

CATIA V5 is utilised here solely for completing the plug geometry profile with the surrounding annular nozzle lip and marking the main CFD domain for surface profile generation. Here, the main emphasis is laid on the parameters controlling external nozzle profile features and not the plug itself. This includes position of throat edge of annular nozzle, back profile limitations, forward CFD hex domain creation for a stable convergent flow analysis, etc. It should be noted that only half of plug geometry is considered, thus ensuring   to meshing efficiency and robustness later on in **ANSYS Fluent**.

Following 2-D surface hex domain for CFD was generated in the form a closed bounded profile:

Figure 5: Complete 2-D CAD profile generated for initial hex mesh layout (CATIA V5)
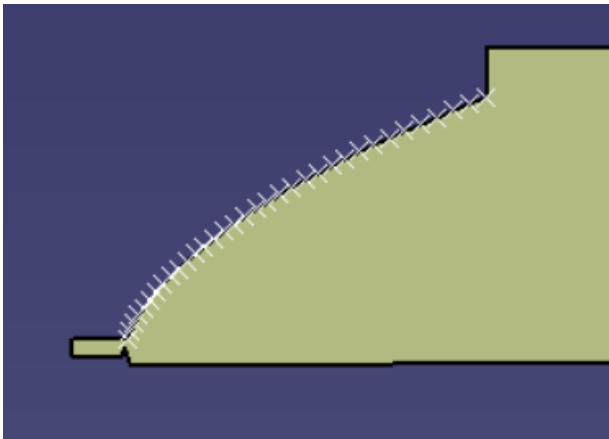
Figure 6: Cross vertices highlighting contour profile points

Important details in the above CAD surface:

(i) The throat of the above contour profile is taken at origin of the CAD surface fill.

(ii) Calculated volumetric space is left in the downstream region so as to ensure complete convergence of the flow later in the Ansys simulation module.

(iii) Only the lower half of the aerospike profile is considered for the CAD surface fill generation and also later for the simulation consideration for lowering computational cost and time.

(iv) The throat design configuration is modulated from the one mentioned and used in ***Chutkey, Kiran et al. (2017)*** where a tilt angle of 55.78 degrees is introduced in the primary nozzle inlet.

(c) 2-D MESH:

Following was the mesh obtained from the Ansys Fluent Meshing module:
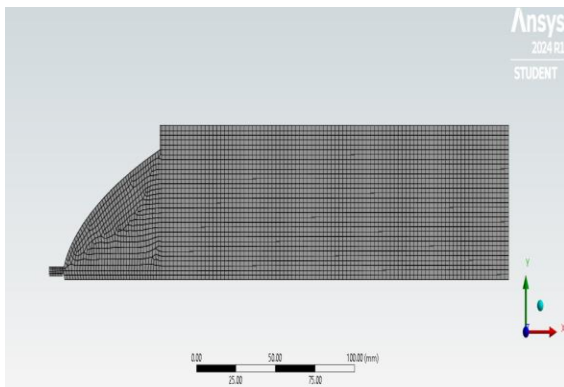
Figure 7: 2-D quadrilateral mesh for the aerospike contour closed profile
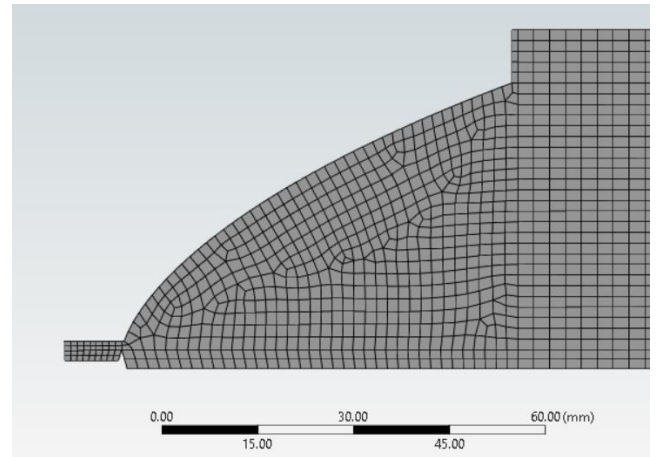
Figure 8: Close up of the aerospike contour wall bound sub-domain mesh

Here a total of 4 sub-domain splits were created in order to maintain meshing efficiency of different regions corresponding to their proximity to the nozzle throat region. The mesh domain splitting, mesh cell shape and size considerations differ from the mesh obtained in ***Chutkey, Kiran et al. (2017)*** wherein a triangular 2-D mesh approach is taken.

Additional information regarding the generated 2-D mesh:

PARAMETER	VALUE/TYPE
Mesh cell shape	Quadrilateral
Mesh cell size range	1.0-2.0 mm
Number of boundaries (total)	5
Number of **inlet** boundaries	1
Number of **outlet** boundaries	1
Number of **symmetry** boundaries	1
Number of **wall** boundaries	2

(d) CFD SIMULATION SET UP & RESULTS:

Following table illustrates the details about the CFD simulation set up parameters including flow material, viscosity equation and solver choices:

PARAMETER	CHOICE/STATUS
Fluid material	Dry air (Ideal gas, Sutherland viscosity)
Inlet velocity	Abs Normal to surface(142.85 m/s^2)
Dynamic mesh	On
RANS viscous equation	Spalart Allmaras (1-eqn)
Solver Method	Simple

Results:

(i) **Pressure profile:**

Observations: The spike in the values occur in the region along the aerospike contour wall since along this region the main expansion of the fluid takes place resulting

in a gradual decrease in the total pressure. In the inlet subsonic domain, the pressure is comparatively higher pertaining to extremity in volume constraints, however the throat still allows a sudden release in the total pressure with ease. The base bleed has a circulation region generated which lowers the pressure from the surrounding higher value stream.
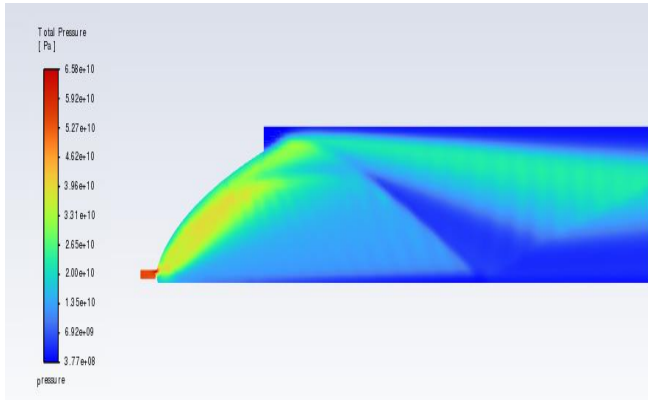
Figure 9: Contour map for Total pressure variation

(ii) Velocity profile:

Observations: The profile in the immediate primary exhaust region is brighter in its velocity value pertaining to expansion reasons. However, a slight shift in the value is seen through transition onto the reddish-orange phase showing that the re-alignment of the velocity vectors takes place at a later stage in the primary exhaust. The shear layer separating the subsonic circulating flow from the primary is also intact and this becomes more and more closed with lower ambient pressure surrounding.
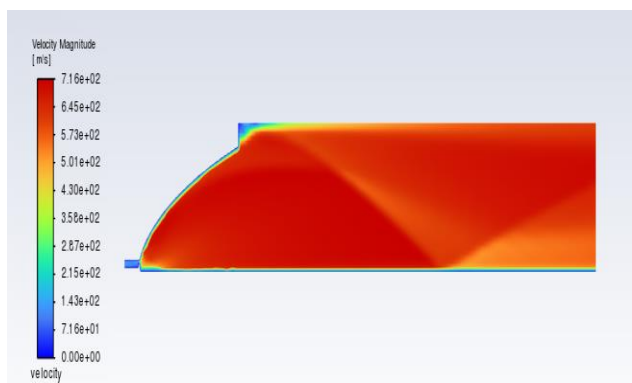
Figure 10: Contour map for velocity magnitude variation

(iii) Velocity Pathway profile around the aerospike wall contour:

Observations: The main reason of inclusion of this pathway profile is to examine the

formation of the subsonic base bleed flow which determines the wake region formation. The flow is continuous in its vortex formation near the flat end of spike base. This pathway profile for higher altitudes becomes more inward streamlined in response to the decrease in ambient pressure.
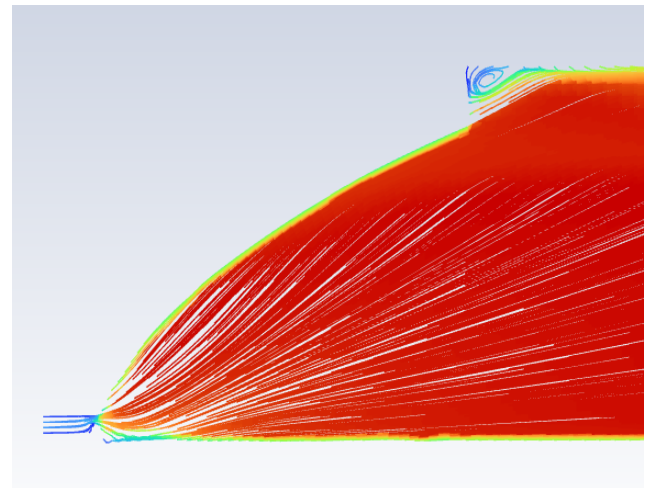
Figure 11: Velocity pathway profile

5.CONCLUSION

The main conclusion is drawn on the difference of the flow obtained in the primary exhaust due to a change in the throat design configuration as compared to the set up in *Chutkey, Kiran et al. (2017),* where the former- sees a wider distribution in pressure and velocity profile due the vertical alignment of the throat lip. This affects the subsonic base bleed region as well as it tends to become slightly more constricted to give an inward bend to the wake region profile. Comparing the wave jet interactions, the said parameter was observed more in the core jet flow in the tilted throat design than in this performance study under reasons directly linked with strong contour profile alignment with the throat lip in *Chutkey, Kiran et al. (2017).* The primary exhaust flow obtained in the current study is evident in its uniformity and less turbidity in its flow. A keen sense of profile judgement was involved in finalising the aerospike contour plug design which also came out as slightly less parabolic as compared to the one designed in *Chutkey, Kiran et al. (2017)* due to algorithm modulations in the current study. The mesh in the original design for this aerospike is much denser around the base bleed and throat lip fissures along with the adjoint domains following a triangular mesh approach whereas the current study uses a quadrilateral mesh approach keeping the fineness under limits to preserve mesh continuity and stability. Finally, the algorithm developed for the aerospike has an additional sub-program which offers changes in the contour design arising from a change in the flying altitude and ambient surrounding parametrization.

6.REFERENCES

1. Chutkey K., Vasudevan N.B., Balakrishnan N., "*Flow field analysis of Linear plug nozzle*", Journal of Spacecraft and Rockets, November 2012.

2. Dakka S., Dennison O., "*Numerical Analysis of Aerospike Engine Nozzle Performance at various truncation lengths*", International Journal of Aviation, Aeronautics, and Aerospace, Volume 8 Issue 2, 2021.

3. Wang C.H., Liu Y., Qin L.Z., "Aerospike nozzle contour design and its performance validation", Acta Astronautica 64, 20 February 2009.

4. Kumara S., Bhaskarb M., Gautamc M., Prakashd B., Kumare S., "*Computational Analysis of 2d Aerospike Nozzle with Base Bleed at Different Altitudes*", Turkish Journal of Computer and Mathematics Education, Vol.12 No.10, 28 April 2021.

5. Sun D., Luo T., and Feng Q., "*New Contour Design Method for Rocket Nozzle of Large Area Ratio*", International Journal of Aerospace Engineering Volume 2019, 20 December 2019.

6. Kumar A., Ogalapur S.G., "*Design of Minimum length nozzle by Method of Characteristics*", 2020.

7. Mishra A.K., Goswami V., "Aerodynamic thrust characteristics and performance valuations for an aerospike nozzle- review", International Journal of Engineering Applied Sciences and Technology, 2021 Vol. 5, Issue 11, March 2021.

8. Imran M., "*Introduction to Aerospike and its Aerodynamic Features*", International Journal of Scientific and Research Publications, Volume 6, Issue 5, May 2016.

9. *Compressible aerodynamics calculator:* https://devenport.aoe.vt.edu/aoe3114/calc.html